

Supplementary material

Manuscript: “Dedicated 3D-T₂-STIR-ZOOMit imaging improves demyelinating lesion detection in the anterior visual pathways of patients with multiple sclerosis”

Emanuele Pravata, MD¹, Luca Roccatagliata, MD,^{2,3} Maria Pia Sormani, PhD^{2,3}, Luca Carmisciano, PhD², Christian Lienerth, MSc.⁴, Rosaria Sacco, MD⁵, Alain Kaelin-Lang, MD^{5,6}, Alessandro Cianfoni, MD^{1,6}, Chiara Zecca, MD*^{5,6}, Claudio Gobbi, MD*^{5,6}

MRI data acquisition and preparation:

Within 4 weeks from clinical assessment, subjects underwent MRI on a 3T Skyra (Siemens, Erlangen, Germany) scanner with a 64-channels head/neck coil. Default B₀-field shimming and patient specific B₁-field shimming were employed. We acquired 3D-T₂-STIR-ZOOMit as well as coronal-plane 2D-T₂-STIR 2.5mm thick images (Table 1). In a randomly chosen subgroup of 12 MS patients, 3D-T₂-STIR-ZOOMit images were re-acquired after patient repositioning, for subsequent “scan-rescan” reproducibility assessment. Voluntary and spontaneous gaze and saccades movements was minimized by asking participants to fixate a target placed on the scanner gantry in front of their eyes (i.e. straight gaze)¹, or alternatively to keep their eyes closed if/when feeling unable to maintain fixation. The scanner room lights were dimmed to improve visual comfort. MRI-compatible eyeglasses were used to adjust for refractive defects, as needed.

Images were transferred to a PC workstation running Linux. In order to improve image signal-to-noise-ratio while preserving small isolated details, an optimized blockwise, non local means denoising filter for 3D MRI images was applied to 3D-T₂-STIR-ZOOMit images (Figure S1)^{2,3}. Finally, images were loaded on a 3D-multiplanar reconstruction (MPR) capable software (FSLEyes, part of the FSL software suite, <https://fsl.fmrib.ox.ac.uk>), and presented to the readers (see corresponding sections in the main text).

References

1. Yiannakas MC, Toosy AT, Raftopoulos RE, Kapoor R, Miller DH, Wheeler-Kingshott CA. Invest Ophthalmol Vis Sci. 2013 Jun 21;54(6):4235-40. doi: 10.1167/iovs.13-12357.
2. Klosowski J, Frahm J. Image denoising for real-time MRI. Magn Reson Med 2017;77(3):1340-1352. doi: 10.1002/mrm.26205
3. Coupe P, Yger P, Prima S, Hellier P, Kervrann C, Barillot C. An optimized blockwise nonlocal means denoising filter for 3-D magnetic resonance images. IEEE Trans Med Imaging 2008;27(4):425-441. doi: 10.1109/tmi.2007.906087

Table S1: Characteristics of participants with multiple sclerosis.

Characteristic	Value
Mean age, (y)*	39.1 (13.1)
Gender (F/M)	30/18
Median disease duration (m)†	91 (22.5, 144)
EDSS (score)†	2.0 (1.5, 3.0)
pON+	19 (39.6)
pON-	29 (60.4)
pON+ Left eye	12 (5.8)
pON+ Right eye	11(5.3)
pON+ Bilateral	4 (8.3)

Note.–Except were indicated, data are numbers of MS participants (n=48) with percentages in parenthesis.

* Number in parenthesis is the standard deviation

† Number in parenthesis is the interquartile range

EDSS=Expanded Disability Status Scale. m=month. pON+=MS participants with acute optic neuritis history. pON-=MS participants without acute optic neuritis history. pON+ Left eye=MS participants with acute optic neuritis history in the left eye. pON+ Right eye=MS participants with acute optic neuritis history in the right eye. pON+ bilateral=MS participants with bilateral acute optic neuritis history.

Table S2. MS participants with and without at least one demyelinating lesion detected with 3D-T₂-STIR-ZOOMit and 2D-T₂-STIR, according to previous AON.

Previous AON	N=48 (100)	3D-T ₂ -STIR-ZOOMit		2D-T ₂ -STIR	
		No lesion	Any lesion	No lesion	Any lesion
No	29 (60.4)	16 (55.2)	13 (44.8)	24 (82.8)	5 (17.2)
Yes	19 (39.6)	1 (5.3)	18 (94.7)	2 (10.5)	17 (89.5)

Note.– Data are numbers of MS participants (N=48) with percentages in parenthesis.

AON = acute optic neuritis.

Supplementary Figures

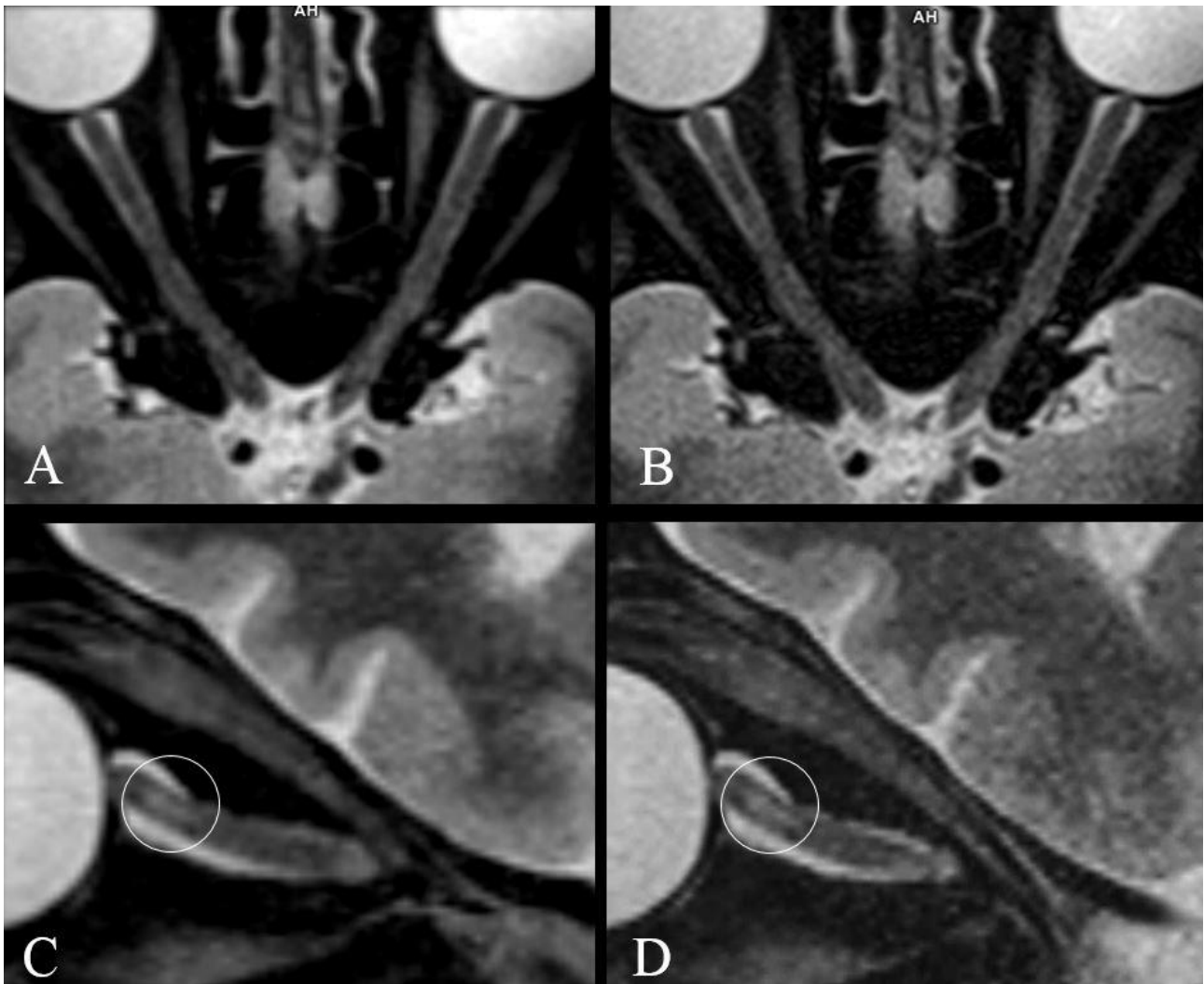


Figure S1. Effect of denoising filter application on 3D-T₂-STIR-ZOOMit images. Same subjects of Figure 1 (HC #9001: A, B – axial plane) and Figure 3 (MS participant #0004: C, D – sagittal-oblique plane), with (A, C) and without (B, D) filtering. Circles in C and D highlight the same small DL.

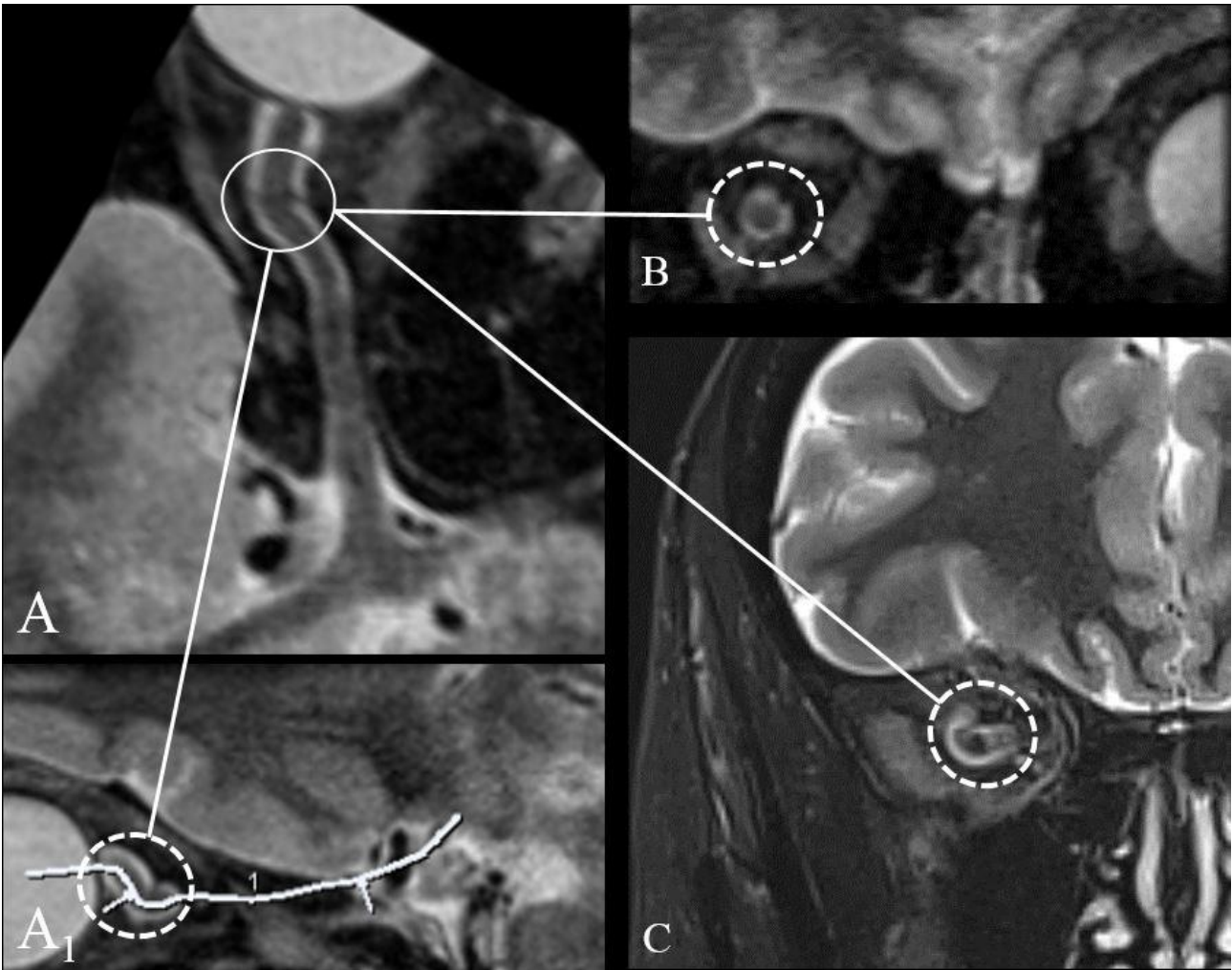


Figure S2. Benefits from the geometrically unbiased 3D evaluation of the aVP anatomy allowed by 3D-T₂-STIR-ZOOMit, in a case of a markedly convoluted optic nerve course. A. Axial curved reconstruction obtained along the right optic nerve true long axis (A₁) in a healthy participant (HC #9021). B. Coronal-oblique reconstruction of 3D-T₂-STIR-ZOOMit image volume shows expected normal optic nerve signal and thickness. B. However, the coronal plane 2D-T₂-STIR image (C) of the same participant and level as B, shows ambiguous signal characteristics related to partial volume effect.

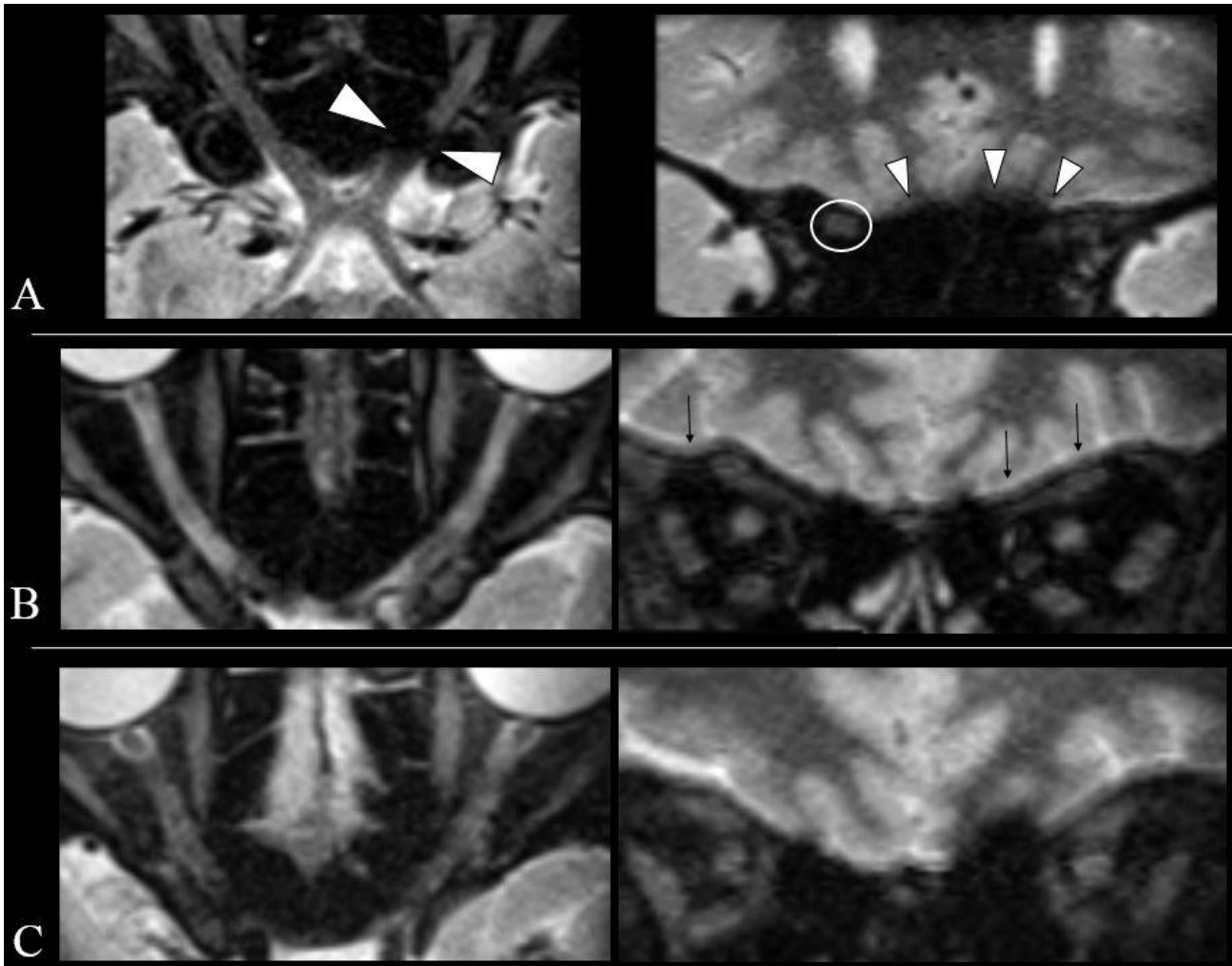


Figure S3. Classification of artifact types and grade for image quality assessment. A. Air-bone interface artifacts at the level of the left optic canal (HC #9002). The left iCanal segment is completely obscured by field inhomogeneity artifact (arrowheads), whereas the contralateral side is normally visible (dashed circle). B. Grade 1 movement artefact. Thin arrows indicate ghosting artefacts with some blurring of the iOrb segment. Hyperintense lesions are seen on both sides (MS participant #0019). C. Grade 2 movement artefacts result in unacceptable image quality (MS participant #0039). The images of this participant were excluded from subsequent analyses.

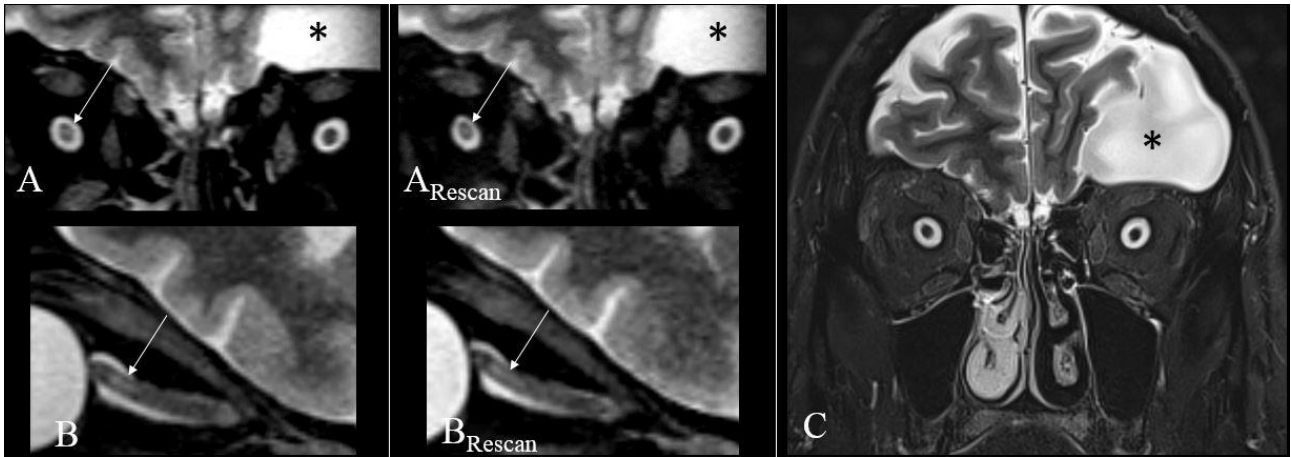


Figure S4. Scan-rescan reproducibility assessment in MS participant #0004). A, A_R shows a very tiny DL located at the center of the R iOrb segment, on coronal, and in B, B_R sagittal-oblique image reconstruction of repeated scans. C. This lesion is not detectable on standard 2D-T₂-STIR images (same level as A, A_R).

*Intracranial arachnoid cyst incidentally noted.